Creep analysis of concrete filled steel tube arch bridges

Y.F. Wang[†], B. Han[‡], J.S. Du[‡†] and K.W. Liu[‡‡]

School of Civil Engineering and Architecture, Beijing Jiaotong University, Beijing 100044, P. R. China

Abstract.   Applying the method calculating creep of Concrete Filled steel Tube (CFT) members based on the Elastic Continuation and Plastic Flow theory for concrete creep with the finite element method, the paper develops a new numerical method for the creep of CFT arch bridges considering effects of bending moment. It is shown that the method is feasible and reasonable through comparing the predicted stresses and deflection caused by the creep with the results obtained by the method of Gu *et al.* (2001) based on ACI209R model and experimental data of an actual CFT arch bridge. Furthermore, nine CFT arch bridges with different types are calculated and analyzed with and without the effects of bending moment. As a result, the bending moment has considerable influences on long-term deformations and internal forces of CFT arch bridges, especially when the section of arch rib is subjected to a large bending moment.

Keywords: creep; CFT; arch bridge; eccentric compression; Finite Element Method (FEM).

1. Introduction

In recent years, CFT arch bridges, which have many advantages, such as favorable mechanical behaviors, convenience to structure construction, aesthetical shapes, as well as good adaptability to variable spans, have been used widely in many countries (Zhong 2003). There are more than 200 CFT arch bridges have been constructed in China. However, as one of the fundamental problems of CFT arch bridges, creep influences on CFT bridges have not been studied adequately.

Creep is a nonelastic deformation of concrete under sustained stress, has considerable influences on arch and some other statically indeterminate structures as pointed by Neville (2002). Creep is often taken into account in structural analysis by incorporating a selected concrete model with the finite element method through transforming the creep strain as the change of geometrical actions, concrete modulus, and internal forces (Murcia 1993, Yan 2004, Cheng 2006). In structural design, the creep coefficient or the creep compliance function, based on a specific concrete creep model, is used to consider the creep effects (Bazant 2001, JGT D62-2004).

For the analysis of the creep of CFT arch bridges, Gu *et al.* (2001), Xie and Qin (2001) carried out primary work on by assuming that the internal forces on arch ribs do not vary during the period of creep development, which is not coincident with actual facts. Additionally, Gu *et al.* (2001)

---

† Professor, E-mail: cyfwang@bjtu.edu.cn
‡ Associate Professor, E-mail: bhan@bjtu.edu.cn
‡† Engineer, E-mail: js.du@rioh.cn
‡‡ Graduate Student, E-mail: mytruelyohye@tom.com

simplified the arch ribs as axial compression members by neglecting influences of bending moment. However, in real engineering, arch ribs always endure not only compression but also bending due to reasons such as different kinds of acting loads, limited arch rise, construction error, and aesthetic requirements. On the basis of the ageing theory of concrete creep, Xin and Xu (2003) presented formulae for calculating the stress redistribution on the cross-sections of the ribs during the core concrete creep. But the ageing theory, which overestimates the concrete creep with decreasing stress (Neville *et al.* 1983), is not suitable for the creep analysis of CFT structures. Besides, the ageing theory was not combined with a numerical method, creep influences on the deformation of CFT arch bridge could not be considered by adopting the method.

Based on the Elastic Continuation and Plastic Flow theory of concrete creep and the creep theory of concrete under multi-axial stresses, considering the mechanical properties of CFT members, Wang (2006), Wang and Han (1999), and Han and Wang (2001, 2004) developed one-dimensional analytical models for creep of CFT members. The models take account of not only characteristics of concrete under multiaxial stresses but influencing factors of creep, e.g. steel ratios, material grades, and stress ratios of CFT members. Moreover, the theory of Elastic Continuation and Plastic Flow based on the concrete rheological model, considering the composition of creep rationally, is suitable to the unloading case of core concrete creep of CFT members. Therefore, the paper combines the mentioned creep model of CFT members under eccentric loads with FEM to propose a new method to analyze the creep of CFT arch bridges.

2. Creep of CFT arch bridges with and without bending moment

Due to the stress distribution is not uniform on each cross-section of CFT members under eccentric loads, and the deformations in different locations of the cross-section are different , the analysis of the members is more complex than that of axial compression members.

Following assumptions for CFT members under eccentric loads are adopted:
(1) CFT is an ideal elastic material;
(2) steel is an ideal elastic material;
(3) creep of core concrete obeys the principle of superposition, i.e. creep is linear;
(4) deformation between steel tube and concrete is compatible;
(5) deformation of members' cross-section satisfies the plane hypothesis.

Generally, under the limitation of serviceability, the confining stress of steel tube to concrete can
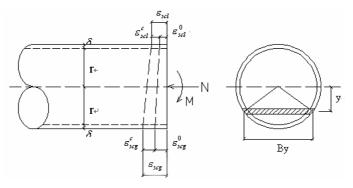

Fig. 1 Cross-section of CFT members under eccentric loading

not occur in arch ribs of CFT arch bridges (Zhong 2003), therefore, the paper does not consider the confining stress in the following analysis.

In the study of creep influence on CFT arch bridges by FEM, the ribs are divided into beam elements without shear force. Here, each element is considered as a member under eccentric force. According to the plane hypothesis, the stress distribution on a cross-section of CFT member under eccentric load is linear along the axis y, and the creep on the cross-section is also linear along the axis, as shown in Fig. 1.

Fig. 1 shows the strain distribution of CFT members under eccentric loading. ε_{scg} denotes the maximum total strain; ε_{scg}^0 is the maximum elastic strain; ε_{scg}^c stands for the maximum creep; ε_{scl} denotes the minimum total creep; ε_{scl}^0 is the minimum elastic strain, ε_{scl}^c stands for the minimum creep; r is the diameter of core concrete; δ is the thickness of steel tube.

The internal force on the cross-section of CFT members under eccentric loading should satisfy the following equilibrium equations

$$\sum N = 0 \tag{1}$$

$$\sum M = 0 \tag{2}$$

i.e.,

$$N_c + N_s = N \tag{3}$$

$$M_c + M_s = M \tag{4}$$

where N_s, N_c--axial force of steel tube and core concrete respectively;

M_s, M_c--bending moment of steel tube and core concrete respectively.

Assume that steel tube and core concrete carry out the internal forces of CFT member according to their stiffness,

$$N_c = N \cdot \frac{E_c \cdot A_c}{E_c \cdot A_c + E_s \cdot A_s} \tag{5}$$

$$N_s = N \cdot \frac{E_s \cdot A_s}{E_s \cdot A_s + E_s \cdot A_s} \tag{6}$$

$$M_c = M \cdot \frac{E_c \cdot I_c}{E_c \cdot I_c + E_s \cdot I_s} \tag{7}$$

$$M_s = M \cdot \frac{E_s \cdot I_s}{E_c \cdot I_c + E_s \cdot I_s} \tag{8}$$

where I_s, I_c- inertia moment of steel tube and core concrete alternatively;

E_s, E_c- Young's modulus of steel tube and concrete alternatively;

A_s, A_c- cross-section area of steel tube and concrete alternatively.

Therefore, the stresses of core concrete and steel tube are

$$\sigma_c = \frac{N_c}{A_c} + \frac{M_c}{I_c} y \tag{9}$$

$$\sigma_s = \frac{N_s}{A_s} + \frac{M_s}{I_s}y \qquad (10)$$

where σ_s, σ_c- axial stress of steel tube, axial stress of core concrete.

According to Eqs. (9) and (10), the stresses of core concrete and steel tube are

$$\sigma_c = N_c\left(\frac{1}{A_c} + \frac{e}{I_c}y\right) \qquad (11)$$

$$\sigma_s = N_s\left(\frac{1}{A_s} + \frac{e}{I_s}y\right) \qquad (12)$$

where $e = \dfrac{M}{N}$.

While the redistribution of stress on the cross-section occurs during creep process, let N_c^c stand for the increment of internal force of core concrete, σ_c^c be the increment of stress; N_s^c stand for the increment of internal force of steel tube, and σ_s^c be the increment of stress, then

$$N_s^c + N_c^c = 0$$

$$\sigma_c^c = N_c^c\left(\frac{1}{A_c} + \frac{e}{I_c}y\right) \qquad (13)$$

$$\sigma_s^c = N_s^c\left(\frac{1}{A_s} + \frac{e}{I_s}y\right)$$

In accordance with the above formulae, it can be obtained that

$$\sigma_s^c = -\frac{\dfrac{1}{A_s} + \dfrac{e}{I_s}y}{\dfrac{1}{A_c} + \dfrac{e}{I_c}y}\sigma_c^c = \frac{1 + \dfrac{A_s e}{I_s}y}{\alpha\left(1 + \dfrac{A_c e}{I_c}y\right)}\sigma_c^c = -\gamma\sigma_c^c \qquad (14)$$

where $\gamma = \dfrac{1 + \dfrac{A_s e}{I_s}y}{\alpha\left(1 + \dfrac{A_c e}{I_c}y\right)}$; α- steel ratio of CFT members, $\alpha = A_s/A_c$.

Under the uni-axial stress, the stresses of steel tube and core concrete have

$$\sigma_s = n\sigma_c \qquad (15)$$

in which n is modulus ratio of steel and concrete, $n = E_s/E_c$.

After the creep occurring, the strain increment of steel tube is

$$\varepsilon_s^c = \frac{\sigma_s^c}{E_s} \qquad (16)$$

and the creep of core concrete is

$$\varepsilon_c^c = \sigma_c c = (\sigma_{c0} + \sigma_c^c)c \qquad (17)$$

where, σ_{c0}- initial stress of core concrete under external force, $\sigma_{c0} = \dfrac{N_{c0}}{A_c} + \dfrac{M_{c0}}{I_c}y$;

c- concrete creep ratio under the uni-axial stress. It can be calculated according to Han and Wang (2001).

Under the assumption of deformation compatibility, $\varepsilon_s^c = \varepsilon_c^c = \varepsilon_{sc}^c$, ε_{sc}^c is the creep of CFT member, and on the basis of Eqs. (16) and (17), there is

$$\varepsilon_{sc}^c = \frac{\sigma_s^c}{E_s} = (\sigma_{c0} + \sigma_c^c)c \tag{18}$$

According to Eqs. (14) and (18), then

$$\sigma_c^c = -\frac{E_s \varepsilon_{sc}^c}{\gamma} \tag{19}$$

Substitute the above formula into Eq. (18), the creep of CFT members under eccentric loading can be obtained along the axis y as following,

$$\varepsilon_{sc}^c = \frac{\sigma_{c0}c}{1 + \dfrac{E_s c}{\gamma}} \tag{20}$$

In order to calculate the creep of points in the section with different distances to the neutral axis, it is assumed that the Young's moduli of arch rib elements are not uniform, and the bigger the creep is, the lower the Young's modulus is relatively, vice versa. It can also be supposed that CFT members under eccentric loading are at the elastic stage during the creep, then the Young's modulus of cross -section in aixs y at time t is

$$E_{sc}^t = \frac{N \cdot \left(\dfrac{1}{A_{sc}} + \dfrac{e}{I_{sc}} \cdot y \right)}{\varepsilon_y^t} \tag{21}$$

where ε_y^t- total strain in coordinate y at time t, $\varepsilon_y^t = \varepsilon_y^0 + \varepsilon_{scy}^c$;

I_{sc}- moment of inertia of CFT member's cross-section, $I_{sc} = I_s + I_c$;

A_{sc}- area of CFT member's cross section, $A_{sc} = A_s + A_c$.

Due to the different Young's modulus in every point with different distance to the neutral axis on the cross section, the transformed moduli of elements after creep can not be directly used in a FEM program as Gu *et al.* (2001) and Xie and Qin (2001), but it needs to integrate the stiffness matrix of element, deducing the transformation element stiffness matrix at each time step during creep.

According to the FEM, consider the increment of cross–sectional Young's modulus, the transformation stiffness matrix of plane bar element is

$$K = \int_A E \, dA \cdot \begin{bmatrix} \dfrac{1}{l} & -\dfrac{1}{l} \\ -\dfrac{1}{l} & \dfrac{1}{l} \end{bmatrix} = \int_{-R}^{R} E_y B_y \, dy \cdot \begin{bmatrix} \dfrac{1}{l} & -\dfrac{1}{l} \\ -\dfrac{1}{l} & \dfrac{1}{l} \end{bmatrix} \tag{22}$$

where E_y- transformation Young's modulus of the CFT member at y;

B_y- cross-section width at y, $B_y = 2\sqrt{R^2 - y^2}$, in which R stands for the core concrete diameter.
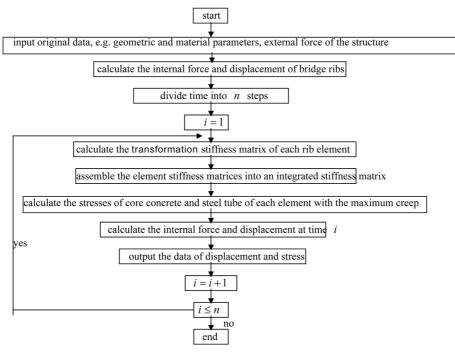
Fig. 2 Flow chart for calculating creep effects of CFT arch bridges

Take into account the increment of cross-sectional Young's modulus, the transformation stiffness matrix of plane beam element without shear force is

$$
K = \int_A E \cdot y^2 dA \cdot \begin{bmatrix} \dfrac{12}{l^3} & \dfrac{6}{l^2} & -\dfrac{12}{l^3} & \dfrac{6}{l^2} \\[2mm] \dfrac{6}{l^2} & \dfrac{4}{l} & -\dfrac{6}{l^2} & \dfrac{2}{l} \\[2mm] -\dfrac{12}{l^3} & -\dfrac{6}{l^2} & \dfrac{12}{l^3} & -\dfrac{6}{l^2} \\[2mm] \dfrac{6}{l^2} & \dfrac{2}{l} & -\dfrac{6}{l^2} & \dfrac{4}{l} \end{bmatrix} = 2\int_A E_y \cdot y^2 \cdot B_y dA \cdot \begin{bmatrix} \dfrac{12}{l^3} & \dfrac{6}{l^2} & -\dfrac{12}{l^3} & \dfrac{6}{l^2} \\[2mm] \dfrac{6}{l^2} & \dfrac{4}{l} & -\dfrac{6}{l^2} & \dfrac{2}{l} \\[2mm] -\dfrac{12}{l^3} & -\dfrac{6}{l^2} & \dfrac{12}{l^3} & -\dfrac{6}{l^2} \\[2mm] \dfrac{6}{l^2} & \dfrac{2}{l} & -\dfrac{6}{l^2} & \dfrac{4}{l} \end{bmatrix} \tag{23}
$$

Combining Eq. (22) with Eq. (23), the transformation stiffness matrix of beam elements of the rib at each creep step can be obtained, and then according to the transformation stiffness matrix, the internal force and deformation of CFT arch bridge after creep (Kwak and Seo 2000, Liao and Zhang 2000) can be calculated by the FEM. The flow chart to implement it is shown as Fig. 2.

3. Examples

Xin and Xu (2003) gave the test results of the creep of Yajisha Bridge, a CFT arch bridge, in Guangdong Province, China. The paper calculates and analyzes the creep of Yajisha Bridge by the
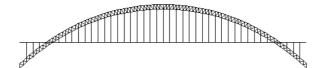
Fig. 3 Structural model of Yajisha CFT arch bridge

presented method and the method proposed by Gu *et al.* (2001) based on ACI209R model, comparing the predicted stresses and deflections caused by creep with the experimental data of Xin and Xu (2003).

The main bridge of Yajisha is a half-through and non-hinged arch bridge with main span of 344 m, arch ribs are designed in a shape of catenary with arch rise 76.45 m, and ratio of rise to span is 1/4.5. Coefficients of arch *m* and *k* are equal to 2 and 1.317 alternatively. Each arch rib is composed with 6 CFTs, which are made of steel tube of Φ750 mm, and is constituted into a CFT truss by connecting with transverse flat plates and web members. Thereinto, the size of outer and inner steel tubes of the truss is Φ750 mm × 18 mm, the size of middle steel tube is Φ750 mm × 20 mm, and the thickness of transverse flat plates between steel tubes is 500 mm. C50 concrete is filled into the tubes of arch ribs and inside between transverse flat plates. More details about the bridge can be seen in Xin and Xu (2003). For the convenience of calculation, the spatial system of the structure is simplified to a plane system, as seen in Fig. 3.

In the following analysis, suppose that all loads are put on the bridge in a lump, creep is not considered during construction period, the loading age of concrete is 28 days, and loads would sustain 560 days. The bridge is divided into 267 nodes and 484 elements. The total deflection and stress of vault section of main arch were measured respectively when the bridge was completed and open to traffic after 1 year, heretofore, the loading age of concrete of arch rib is approximately 18 months (Xin and Xu 2003). The experimental data and results gotten by the two methods without considering bending moment are listed in Table 1.

According to Table 1, it can be shown that there are some differences between numerical results and experimental data when the bridge was completed, and the deference in steel tube stresses between the calculated results and experimental data are about 15% and 21%, and concrete stresses are about 31% and 21% for the results of the paper and Gu *et al.* (2001) respectively. The reasons are related to the factors such as the modelling simplification, ignoring the creep during construction as well as bending monents. After the bridge was operated 1 year, the discrepancies of steel tube and core concrete stresses between numerical results and experimental data are 10% and 14% as well as 49% and 47% respectively, and the deflections have dispersions about 12% and 7%. It can be concluded that the calculated results agree well with the experimental data.

Table 1 Comparison of predicted deflections and stress of vault section with experimental data

Contents	Location	Experimental data	Results of this paper	Gu *et al.* (2001)
Stresses of upside of the vault when bridge was completed (MPa)	steel	206.4	237.8	248.9
	concrete	13.8	18.2	16.8
Stresses of upside of the vault after the bridge was operated 1 year (MPa)	steel	218.3	239.2	250.6
	concrete	11.3	16.8	16.6
Total deflection caused by creep (cm)		12.0	13.7	12.8

Concrete stress curves   Stress curves of steel tube rib

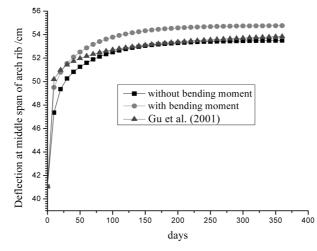Fig. 4 Stress curves at mddle span of arch rib

Fig. 5 Deflection curves at middle span of arch rib

The stress and deformation curves of Yajisha Bridge obtained by the method of Gu *et al.* (2001) without bending moment and the paper's method with and without bending moment are shown as Figs. 4, 5. From Table 1 and the figures, it can be seen that the stresses and deflections of the bridge after 1-year creep obtained by the two methods are close to each others, but for results on the early stage and the creep development, the presented method has a better description than that of the method proposed by Gu *et al.* (2001) based on ACI209R model.

As shown in the curves obtained by the two methods with and without bending moment , it can be concluded that the deflection of CFT arch ribs will increase with creep developing. These curves change obviously in early time, after 60 days, the curves will develop slowly, be close to horizontal lines after 180 days, and almost terminate after 360 days. The increment of the deflection is about 30% of its initial value. The deflection increment of the middle span with bending moment is 10% bigger than that without bending moment. Stresses of core concrete and steel tube with bending moment are also 20% larger than that without bending moment. In addition, concrete stresses have

been decreasing during creep, while steel tube stresses increasing.

Based on the above work, in order to analyze the creep effects on arch bridges with different types and spans as well as the effects of moment on the creep of CFT bridge, nine different CFT arch bridges, shown as in Table 2, are chosen and calculated respectively by using two methods with and without considering bending moments.

For the purpose of comparison, calculated results such as deflections and stresses of some important positions of 9 samples are listed from Table 3 to Table 7. Table 3 shows that after 360 days the creep occurred, the deflection at middle span with bending moment is bigger than that without bending moment, but the increments are small: the most is about 8.29% and the least is 2.38%. In addition, it can also be shown in Table 3 that bridge 3 and bridge 4 with small ratio of rise-span have bigger increments of deflections. That indicates that arch shapes will affect the creep of CFT arch bridges. While the arch is designed to endure moments, the influences of creep on the deflection of CFT arch bridge will increase accordingly.

Table 3 to Table 7 indicate that the maximum stresses of core concrete and steel tube vary to some extent after 1-year creep. Because of bearing larger bending moment at arch string than that at

Table 2 Basic parameters of nine calculated models

| No. | Span (m) | Ratio of rise-span | Arch shape | Structure type | Configuration of arch rib | | | Concrete grade |
					Constitution	Height (m)	Dimension (mm × mm)	
bridge.1	85	1/4	quadratic parabola	half-through	three-limb truss	2.5	650 × 12	C50
bridge.2	160	1/5	catenary m=1.543	deck-type	dumb-bell	2.5	1000 × 10	C50
bridge.3	115	1/6	catenary m=1.347	through-type	dumb-bell	2	800 × 10	C30
bridge.4	100	1/9.6	quadratic parabola	half-through	Single tube	0.65	650 × 10	C30
bridge.5	120	1/4	quadratic parabola	half-through	dumb-bell	2	900 × 10	C40
bridge.6	76	1/4	quadratic parabola	half-through	dumb-bell	1.9	800 × 10	C40
bridge.7	46	1/3	quadratic parabola	half-through	Single tube	0.8	800 × 14	C50
bridge.8	160	1/5	catenary m=1.5	through-type	dumb-bell	3.75	1500 × 16	C50
bridge.9	360	1/4.5	catenary m=2	half-through	six-limb truss	6.75	750 × 18	C50

Table 3 Deflection at middle span- comparison of results of two methods

No.	Deflection before creep (without bending moment) (MPa)	Deflection before creep (with bending moment) (MPa)	Deflection after creep (without bending moment) (MPa)	Deflection after creep (with bending moment) (MPa)	Ratio (%)
bridge.1	25.14	38.78	39.92	1.14	2.94
bridge.2	59.64	90.60	94.40	3.80	4.19
bridge.3	52.79	69.68	74.65	4.96	7.12
bridge.4	54.08	72.60	78.62	6.02	8.29
bridge.5	26.15	37.71	40.33	2.62	6.95
bridge.6	20.96	30.21	31.69	1.47	4.87
bridge.7	5.71	9.02	9.42	0.40	4.44
bridge.8	45.63	69.37	72.25	2.88	4.15
bridge.9	410.74	534.89	547.62	12.73	2.38

Table 4 Concrete stress at middle span-comparison of results of two methods

No.	Stresses before creep (without bending moment) (MPa)	Stresses before creep (with bending moment) (MPa)	Stresses after creep (without bending moment) (MPa)	Stresses after creep (with bending moment) (MPa)	D-value (MPa)	Ratio (%)
bridge1	11.32	13.55	9.93	10.49	0.56	5.7
bridge.2	6.59	7.57	5.80	6.65	0.85	14.6
bridge.3	5.95	6.85	5.04	5.83	0.79	15.8
bridge.4	5.64	6.29	4.65	5.12	0.48	10.2
bridge.5	5.98	6.33	4.95	5.24	0.29	5.9
bridge.6	6.36	6.72	5.42	5.73	0.31	5.8
bridge.7	3.89	4.77	3.08	3.73	0.65	21.1
bridge.8	5.25	6.12	4.61	5.36	0.75	16.3
bridge.9	22.50	25.88	14.06	16.81	2.74	19.5

Table 5 Steel tube stress at middle span-comparison of results of two methods

No.	Stresses before creep (without bending moment) (MPa)	Stresses before creep (with bending moment) (MPa)	Stresses after creep (without bending moment) (MPa)	Stresses after creep (with bending moment) (MPa)	D-value (MPa)	Ratio (%)
bridge1	56.75	70.85	86.46	105.51	19.05	22.0
bridge 2	36.24	42.28	55.41	64.24	8.83	15.9
bridge 3	49.57	56.04	66.34	75.31	8.97	13.5
bridge 4	44.99	49.65	60.36	66.56	6.21	10.3
bridge5	37.73	40.09	54.09	57.40	3.31	6.1
bridge6	41.41	43.81	59.33	62.74	3.41	5.7
bridge7	19.67	25.23	29.99	37.54	7.56	25.2
bridge8	28.83	34.21	44.08	51.93	7.85	17.8
bridge9	158.59	183.62	207.74	239.18	31.44	15.1

Table 6 Concrete stress at arch springing- comparison of results of two methods

No.	Stresses before creep (without considering bending moment) (MPa)	Stresses before creep (considering bending moment) (MPa)	Stresses after creep (no considering bending moment) (MPa)	Stresses after creep considering bending moment) (MPa)	D-value (MPa)	Ratio (%)
bridge1	10.34	17.19	7.67	12.78	5.10	66.5
bridge2	8.40	9.32	7.39	8.20	0.81	10.9
bridge3	7.06	7.54	5.99	6.43	0.44	7.4
bridge4	6.06	7.29	4.99	5.89	0.90	18.1
bridge5	8.09	8.76	6.69	7.24	0.55	8.2
bridge6	8.72	9.41	7.42	8.02	0.60	8.1
bridge7	6.13	9.19	4.83	7.02	2.19	45.2
bridge8	6.67	7.40	5.87	6.49	0.63	10.7
bridge9	25.02	29.04	15.02	18.65	3.63	24.2

Table 7 Stress of steel tube at arch springing-comparison of results of two methods

No.	Stresses before creep (without bending moment) (MPa)	Stresses before creep (with bending moment) (MPa)	Stresses after creep (without bending moment) (MPa)	Stresses after creep (with bending moment) (MPa)	D-value (MPa)	Ratio (%)
bridge1	51.84	95.10	78.99	137.30	58.31	73.8
bridge2	46.17	51.92	70.58	78.99	8.41	11.9
bridge3	58.81	62.27	78.70	83.50	4.80	6.1
bridge4	48.31	57.23	64.81	76.68	11.87	18.3
bridge5	51.04	55.49	73.16	79.40	6.24	8.5
bridge6	56.81	61.38	81.39	87.87	6.48	8.0
bridge7	31.05	50.37	47.33	73.55	26.22	55.4
bridge8	36.66	41.15	56.04	62.59	6.55	11.7
bridge9	176.37	206.11	229.42	268.25	38.83	16.9

middle span, the stress variation of core concrete and steel tube at arch string is greater than that at middle span.

4. Conclusions

(1) Curves of stress and deflection of CFT arch bridges influenced by the creep develop rapidly in early age and then slowly. Trends of the curves are nearly horizontal after 180 days, and changes almost terminate after 360 days.

(2) After 360-day creep, calculated deflections and stresses of concrete and steel tube with bending moment are comparatively bigger than that without bending moment. The curves of stress and deflection of CFT arch bridges under long-term loads with and without bending moment have the same trends.

(3) Generally, there are bending moments on arch ribs, creep effects on the stresses of steel tube and concrete of the ribs are bigger. The influence of bending moment on the creep of CFT arch bridge must be taken into account.

Acknowledgements

References

Bazant, Z.P., Xi, Y., Baweja, S. and Carol, I. (1993), "Preliminary guidelines and recommendation for characterizing creep and shrinkage in structural design codes", *Creep and Shrinkage of Concrete*, edited by

Bazant, Z.P. and Carol, I. (1993), E & FN Spon, London, 805-830.

Chen, B.C. (1999), *Design and Construction of CFT Arch Bridges*, Renmin Jiaotong Press, Beijing.

Cheng, X.D., Cheng, L.S. and Ye, G.R. (2006), "Creep analysis of steel concrete composite girder bridges by the method of 3 D-VLE", *Chinese J. Comput. Mech.,* **23**(4), 470-475.

Gu, J.Z., Liu, X.L. and Chen, W.F. (2001), "Analysis of CFT arch bridges considering creep", *J. Shanghai Jiaotong University*, **35**(10), 1574-1577.

Han, B. and Wang, Y.F. (2001), "Creep analysis of small eccentrically compressed CFT members", *Eng. Mech.*, **18**(6), 110-116.

Han, B. and Wang, Y.F. (2004), "Long term load-carrying capacity of axially compressed Concrete Filled Steel Tubular short columns", *Proc. of '04 ISCC,* Changsha.

Kwak, H.G. and Seo, Y.J. (2000), "Long-term behavior of composite girder bridges", *Comput. Struct.*, **74**, 583-599.

Liao, L. and Zhang, N. (2000), "Finite element method of concrete shrinkage and creep", *Ordnance Transaction*, **21**, 32-34.

Murcia, J. (1993), "Analysis of creep and shrinkage as geometrical actions in evolving and nonevoling structures", *Creep and Shrinkage of Concrete,* edited by Bazant, Z.P. and Carol, I. (1993), E & FN Spon, London, 543-544.

Neville, A.M., Dilger, W.H. and Brooks, J.J. (1983), *Creep of Plain and Structure Concrete*, Construction Press, New York.

Neville, A.M. (2002), "Creep of concrete and behavior of structures-Part I: Problems", *Concrete Int.,* **24**(5), 59-66.

Wang, X.C. and Shao, M. (1995), *Fundamentals and Numerical Method of FEM*, Tsinghua University Press, Beijing.

Wang, Y.F. and Han, B. (1999), "Creep analysis of axially compressed Concrete Filled Steel Tubular members", *Proc. of EPMESC VII*, Macao.

Wang, Y.F. (2006), *Creep of Concrete Filled Steel Tube*, Science Press, Beijing.

Xie, X.L. and Qin, R. (2001), "Theoretical research of shrinkage and creep's influence on CFT arch bridges", *Bridge Constr.*, **4**, 1-4.

Xin, B. and Xu, S.Q. (2003), "Creep analysis of long-span CFT arch bridges", *Railway Standard and Design*, **4**, 31-33.

Yan, D.H., Tian, Z.C., Li, X.W. and Tu, G.Y. (2004), Finite element method and application for the shrinkage and creep of concrete bridges, *China J. Highway and Transport*, **17**(2), 55-58.

Zhong, S.T. (2003), *Concrete Filled Steel Tubular structures (3rd edition)*, Tsinghua University Press, Beijing.